PROCEEDINGS OF SCIENCE

Symmetry breaking and clock model interpolation in 2D classical O(2) spin systems

Leon Hostetler,[a,*] **Ryo Sakai,**[b] **Jin Zhang,**[c] **Alexei Bazavov**[a] **and Yannick Meurice**[d]

[a] *Michigan State University,*
East Lansing, Michigan 48824, USA
[b] *Jij Inc.,*
Bunkyo-ku, Tokyo 113-0031, Japan
[c] *Chongqing University,*
Chongqing 401331, People's Republic of China
[d] *The University of Iowa,*
Iowa City, Iowa 52242, USA
E-mail: hostet22@msu.edu, r.sakai@j-ij.com, jin-zhang@uiowa.edu, bazavov@msu.edu, yannick-meurice@uiowa.edu

Motivated by attempts to quantum simulate lattice models with continuous Abelian symmetries using discrete approximations, we study an extended-O(2) model that differs from the ordinary O(2) model by the addition of an explicit symmetry breaking term. Its coupling allows to smoothly interpolate between the O(2) model (zero coupling) and a q-state clock model (infinite coupling). In the latter case, a q-state clock model can also be defined for noninteger values of q. Thus, such a limit can also be considered as an analytic continuation of an ordinary q-state clock model to noninteger q. In previous work, we established the phase diagram of the model in the infinite coupling limit. We showed that for noninteger q, there is a second-order phase transition at low temperature and a crossover at high temperature. In this work, we establish the phase diagram at finite values of the coupling using Monte Carlo and tensor methods. We show that for noninteger q, the second-order phase transition at low temperature and crossover at high temperature persist to finite coupling. For integer $q = 2, 3, 4$, there is a second-order phase transition at infinite coupling (i.e. the clock models). At intermediate coupling, there are second-order phase transitions, but the critical exponents vary with the coupling. At small coupling, the second-order transition for $q = 4$ may turn into a BKT transition.

The 40th International Symposium on Lattice Field Theory (Lattice 2023)
July 31st - August 4th, 2023
Fermi National Accelerator Laboratory

*Speaker

© Copyright owned by the author(s) under the terms of the Creative Commons Attribution-NonCommercial-NoDerivatives 4.0 International License (CC BY-NC-ND 4.0).

PoS(LATTICE2023)223

1. Introduction

Studying quantum field theories at finite density and real time is an extremely hard problem for classical computers. Conventional methods suffer from severe sign problems which make real-time dynamics completely out of reach unless we use a new approach such as quantum simulation. As a first step, we might consider low-dimensional Abelian models such as the Abelian-Higgs model in $(1 + 1)$ dimensions which can in principle be mapped to a Rydberg ladder simulator [1–4]. The Abelian-Higgs model reduces to the classical O(2) model in the limit of infinite self-coupling and zero gauge coupling. Thus the analog simulation of an O(2)-like model may be a good first step toward the simulation of the Abelian-Higgs model.

For a lattice gauge theory, the continuous gauge degrees of freedom give rise to an infinite-dimensional Hilbert space at each link, and this poses a problem for quantum simulation in practice. One possibility is to truncate the Hilbert space at each link in some controlled manner that preserves some of the symmetries of the field. For example, in the Abelian-Higgs model, the U(1) gauge fields may be approximated with $\mathbb{Z}_q$ discrete degrees of freedom. To optimize such an approximation it will be useful to have a continuous family of models that interpolate among the various $\mathbb{Z}_q$ approximations.

We study the effect of explicitly broken symmetries in classical O(2) spin systems in $(1 + 1)$ dimensions by adding a symmetry-breaking term $-h_q \sum_x \cos(q\varphi_x)$ to the action of the ordinary O(2) model. When $h_q > 0$, the O(2) symmetry is broken down to a $\mathbb{Z}_q$ symmetry, and in the limit $h_q \to \infty$, the q-state clock models are recovered. When q is noninteger, the $\mathbb{Z}_q$ symmetry is further reduced to a $\mathbb{Z}_2$ symmetry. The symmetry-breaking term allows to continuously interpolate between the O(2) model ($h_q = 0$) and the q-state clock models ($h_q \to \infty$) by varying h_q and to continuously interpolate between different clock-like models by fixing h_q and varying q. By establishing the phase diagram of this model, we may gain some insight into the challenges faced in approximating U(1) gauge fields with $\mathbb{Z}_q$ discrete degrees of freedom. Early results suggested a phase diagram similar to that found in Rydberg atom chains, however, this was not supported by further investigation. The model is studied using both Monte Carlo (MC) and tensor renormalization group (TRG) methods—serving as a playground for the development of tensor methods and highlighting some of the advantages and disadvantages of these two approaches. More details of this study can be found in our recently posted preprint [5].

2. The Extended-O(2) Model

We consider a classical spin system in $(1 + 1)$ dimensions with energy function

$$S = -\sum_{x,\mu} \cos(\varphi_{x+\hat{\mu}} - \varphi_x) - h_q \sum_x \cos(q\varphi_x), \tag{1}$$

We call this the "Extended-O(2)" model since it is formed by adding a symmetry-breaking term $-h_q \sum_x \cos(q\varphi_x)$ to the ordinary O(2) model. The two-component unit vector sitting on the lattice site x is parameterized with a single angle $\varphi_x \in [0, 2\pi)$. The partition function is

$$Z = \int_0^{2\pi} \prod_x \frac{d\varphi_x}{2\pi} e^{-\beta S}. \tag{2}$$

PoS(LATTICE2023)223

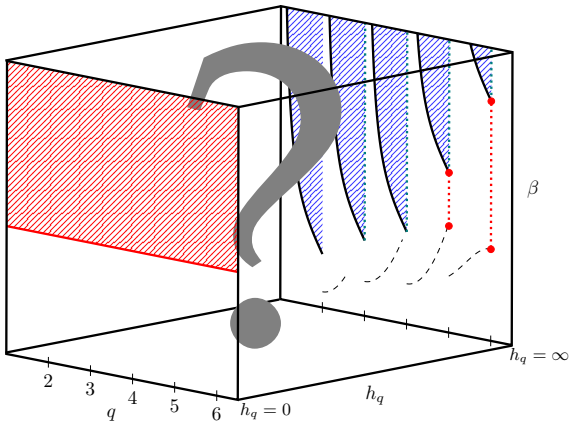

Figure 1: The uncompleted phase diagram of the Extended-O(2) model [6]. At $h_q = 0$, the model reduces to the ordinary O(2) model for all values of q, with a disordered phase at small β, a BKT transition near $\beta_c = 1.12$, and a critical phase at $\beta \geq \beta_c$. For $h_q \to \infty$, the model reduces to the q-state clock model. For $q = 2, 3, 4$, there is a second-order phase transition, and for integer $q \geq 5$, there seem to be two BKT transitions. For noninteger values of q, we find a second-order phase transition of the 2D Ising universality class. The goal of the present work is to establish the phase diagram for this model at finite h_q.

The Extended-O(2) model has two continuously tunable symmetry-breaking parameters q and h_q. When $h_q = 0$, it reduces to the ordinary O(2) model, but when $h_q > 0$, the $O(2)$ symmetry is broken down to a $\mathbb{Z}_q$ symmetry, and the system starts to behave like a clock model. In the limit $h_q \to \infty$, the angles are forced into the clock angles

$$0 \leq \varphi = \frac{2\pi k}{q} < 2\pi. \tag{3}$$

For integer q, the result is the ordinary q-state clock model. For noninteger q, this defines an interpolation of the clock model to noninteger values of q. We previously characterized the phase diagram of this model in the clock model limit ($h_q \to \infty$) [6, 7]. See Fig. 1. For noninteger values of q, the $\mathbb{Z}_q$ symmetry is reduced to a $\mathbb{Z}_2$ symmetry, and we find a single phase transition of the 2D Ising universality class.

The goal of the present work is to establish the phase diagram of the Extended-O(2) model at finite h_q. Specific cases of this model for finite h_q and integer q have been studied before. The model with $q = 2, 3, 4$ seems to be of particular interest. For $h_q \to \infty$, these are the q-state clock models with a second-order phase transition. In particular, $q = 2, 4$ are of the 2D Ising universality class. At finite h_q, there is some evidence that the critical exponents for $q = 2, 3, 4$ vary with h_q, i.e. there are second-order phase transitions but they are no longer in the same universality class as the clock models [8–12]. There is also some evidence that these turn into BKT transitions at sufficiently small but positive h_q [9, 13], although there are others who disagree [14, 15]. In this work, we study the model at finite h_q using MC and TRG across a wide range of integer and noninteger q to characterize the phase diagram. Preliminary findings were presented in [16]. In the present work, we were able to confirm that for $q = 3, 4$, the critical exponents vary with h_q. We find evidence that the second-order transition for $q = 4$ turns into a BKT transition at small but finite h_q. For noninteger q, the model at finite h_q appears to be the same as the model in the $h_q \to \infty$ limit. That

PoS(LATTICE2023)223

is, there is a single second order transition of the 2D Ising class. More details can be found in the Ph.D. thesis [17] and in the recently posted preprint [5].

We measure the specific heat

$$C_V = \frac{-\beta^2}{V}\frac{\partial\langle E\rangle}{\partial\beta} = \frac{\beta^2}{V}(\langle E^2\rangle - \langle E\rangle^2), \tag{4}$$

where the internal energy is defined to be $\langle E\rangle = \langle S\rangle$, and $\langle \dots \rangle$ denotes the ensemble average and $V = L^2$ is the lattice volume. For the MC simulations, we use zero external magnetic field, and measure a proxy magnetization

$$\langle|\vec{M}|\rangle = \left\langle \left| \sum_x \vec{S}_x \right| \right\rangle. \tag{5}$$

where $\vec{S}_x$ is the two-component unit vector sitting at the lattice site x. The corresponding magnetic susceptibility is

$$\chi_{|\vec{M}|} = \frac{1}{V}\left(\langle|\vec{M}|^2\rangle - \langle|\vec{M}|\rangle^2\right), \tag{6}$$

and the Binder cumulant is

$$U_{|\vec{M}|} = 1 - \frac{\langle|\vec{M}|^4\rangle}{3\langle|\vec{M}|^2\rangle^2}. \tag{7}$$

We also measure the structure factor

$$F(\vec{p}) = \frac{1}{V}\left\langle \left| \sum_j e^{-i\vec{p}\cdot\vec{x}_j}\vec{S}_j \right|^2 \right\rangle, \tag{8}$$

where $\vec{x}_j$ is the 2-component Cartesian vector corresponding to the jth lattice site. We considered momenta $\vec{p} = 2\pi\vec{n}/L$, with $\vec{n} \in \{(0,0),(1,0),(2,0),\dots,(L/2,0)\}$.

3. Phase Diagram at Finite-h_q

As a first step, we measured several observables across a large range of the parameter space. In Fig. 2 (top row), we show heatmaps from TRG of the specific heat at $h_q = 1.0$ and $h_q = 0.1$. Since the specific heat often diverges at a critical point, such a heatmap can serve as a proxy for the phase diagram. We see smooth connecting lines even across integer values of q, suggesting a phase diagram where the discontinuities seen for $h_q \to \infty$ (see Fig. 1) become smooth curves for finite h_q. These heatmaps are reminiscent of the phase diagram of a quantum simulator composed of Rydberg atoms [18, 19]—a system which also has several continuously tunable parameters and exhibits various $\mathbb{Z}_q$ symmetries. However, a look at the entanglement entropy, Fig. 2 (bottom row), suggests a different picture with obvious discontinuities at integer values of q.

PoS(LATTICE2023)223

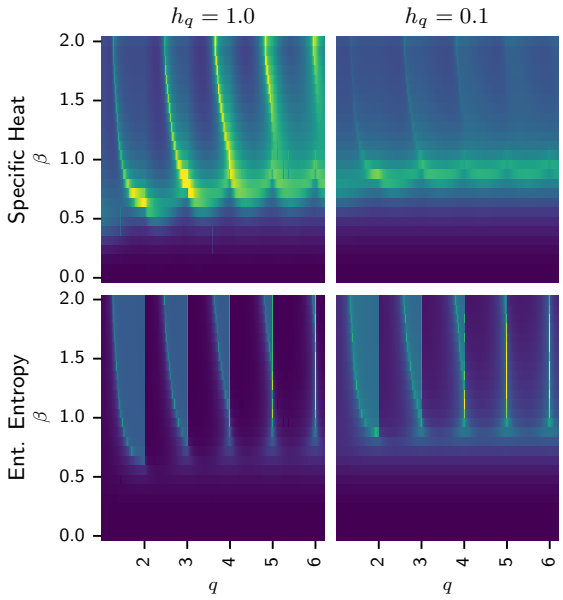

Figure 2: In the top row we show heatmaps from TRG of the specific heat for the Extended-O(2) model at finite h_q. These serve as a proxy for the phase diagram and suggest smoothly connected lines in the phase diagram. However, the entanglement entropy (bottom row) shows discontinuities at integer values of q reminiscent of the phase diagram in the limit $h_q \to \infty$. Each pixel in this figure is from a TRG calculation performed with $L = 1024$ and bond dimension 40.

To establish the actual phase diagram we completed a finite-size scaling analysis with the following fit forms:

$$\left.\frac{dU_{|\vec{M}|}}{d\beta}\right|_{max} = U_0 + U_1 L^{1/\nu} \tag{9}$$

$$C_V|_{max} = C_0 + C_1 L^{\alpha/\nu} \tag{10}$$

$$\left.\langle|\vec{M}|\rangle\right|_{infl} = M_0 + M_1 L^{-\beta/\nu} \tag{11}$$

$$\left.\chi_{|\vec{M}|}\right|_{max} = \chi_0 + \chi_1 L^{\gamma/\nu} \tag{12}$$

$$F(\vec{p})|_{max} = F_0 + F_1 L^{2-\eta}, \tag{13}$$

where $|_{max}$ means evaluated at the maximum and $|_{infl}$ means evaluated at the inflection point. When $\alpha = 0$, as it is for transitions of the 2D Ising universality class, Eq. (10) is modified to

$$C_V|_{max} = C_0 + C_1 \ln L. \tag{14}$$

For noninteger q, we generally see two peaks in a plot of the specific heat versus β. In previous work [6, 7], we found that in the $h_q \to \infty$ limit, the peak at small β is associated with a crossover, whereas the peak at larger β is associated with an Ising phase transition. In the present work, we consider the same noninteger values of q but now at finite h_q. For noninteger q, the explicitly broken $\mathbb{Z}_q$ symmetry caused difficulties for the MC approach resulting in large autocorrelations which made a finite-size scaling analysis impractical with that approach. With TRG there were no

PoS(LATTICE2023)223

q	h_q	ν	α	β	γ	η
2	0.1	1.044(53)	0.021(18)	0.319(94)	1.859(96)	0.287(13)
2	1.0	1.022(71)	-0.010(16)	N/A	1.78(12)	0.251(14)
3	0.1	0.658(24)	0.354(35)	N/A	1.291(45)	0.3651(93)
3	1.0	0.809(26)	0.311(21)	N/A	1.411(36)	0.295(16)
4	0.1	2.49(89)	-0.30(12)	0.76(87)	4.3(1.5)	0.2570(85)
4	1.0	1.20(14)	-0.162(19)	0.78(61)	2.09(24)	0.2532(93)
5	0.1	N/A	N/A	N/A	N/A	0.2716(72)
5	1.0	N/A	N/A	N/A	N/A	0.2653(94)
6	0.1	N/A	N/A	N/A	N/A	0.2880(86)
6	1.0	N/A	N/A	N/A	N/A	0.2654(92)

Table 1: The first two columns refer to the model parameters, and the remaining columns list the critical exponents obtained for the model. They are obtained via the finite-size-scaling ansätze given in Eq. (9)–(14). Some exponents could not be extracted reliably from our data. For $q = 5, 6$, we were able to obtain good estimates only for the exponent η. This is because $q = 5, 6$ have infinite order BKT transitions for which ν is not well defined, and our method of extracting the bare exponents listed here depends on an estimate of ν obtained via Eq. (9). This may also be why we see large error bars for the case $q = 4$, $h_q = 0.1$, which we argue in the main text shows characteristics of a BKT rather than a second-order transition. Note, for $q = 5, 6$ there are two phase transitions. The results listed here refer to the transition at high temperature.

such problems, and we studied the specific heat and magnetic susceptibility for some representative values of q on lattices up to $L = 1024$. For sufficiently large volumes, we find that the magnetic susceptibility plateaus for the small-β peak—implying a crossover—whereas for the large-β peak the susceptibility and specific heat diverge with critical exponents of the 2D Ising universality class. We conclude that the phase diagram for noninteger q in the clock model limit ($h_q \to \infty$) persists to finite $h_q > 0$.

For integer q the model retains a rotational symmetry and the autocorrelations in the MC approach remain manageable. A biased Metropolis heatbath algorithm was used with saved measurements separated by 2^6 or more discarded measurements. Any remaining autocorrelation was removed by binning the observables. We studied the model with $q = 2, 3, 4, 5, 6$, $h_q = 0.1, 1$, and with lattice sizes up to $L = 256$. Using the FSS fit forms given in Eq. (9)–(14), we extracted the exponents $1/\nu$, α/ν, $-\beta/\nu$, γ/ν, and $2-\eta$ and used them to estimate the critical exponents $\nu, \alpha, \beta, \gamma$, and η. In the clock model limit ($h_q \to \infty$), there is a second-order phase transition when $q = 2, 3, 4$ and a pair of BKT transitions when $q \geq 5$. In particular, for $q = 2, 4$, the transition is of the 2D Ising class. We start with the assumption that the same critical behavior persists to finite h_q.

At finite h_q, we find for $q = 5, 6$ two phase transitions consistent with BKT as in the $h_q \to \infty$ limit. Near both critical points, the magnetic susceptibility diverges with increasing volume whereas the specific heat plateaus. Fits to Eq. (9) were unstable, and so we were unable to extract a reliable estimate for the critical exponent ν. This is because for BKT transitions the exponent ν is not well defined. This also meant we were unable to estimate the bare exponents α, β, and γ. Our estimates for η are shown in Table 1. For $q = 3, 4$, we find that at intermediate h_q there is a second-order phase

PoS(LATTICE2023)223

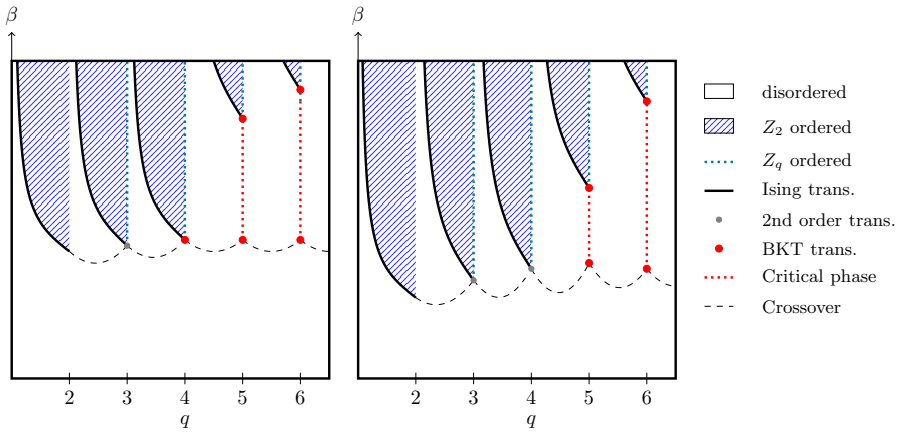

Figure 3: Here we present two-dimensional scenarios of the full three-parameter phase diagram for small h_q (left panel) and intermediate h_q (right panel). At intermediate h_q, we see the same general picture as we see in the limit $h_q \to \infty$ (see Fig. 1). That is, for noninteger q, there is a crossover at small β and an Ising phase transition at larger β. The most significant difference is that the second-order phase transition at $q = 4$ is no longer in the 2D Ising universality class. At small h_q, the picture at noninteger q stays nearly the same albeit with a shift to larger β. We find evidence that the second-order transition for $q = 4$ turns into a BKT transition at small h_q.

transition that varies with the coupling h_q and so the transition is no longer in the same universality class as the q-state clock models ($h_q \to \infty$ limit). For example, for $q = 3$, the $h_q \to \infty$ limit is in the universality class of the 3-state Potts model with critical exponent $\gamma = 13/9$. When $h_q = 1$ we find $\gamma = 1.411(36)$, but when $h_q = 0.1$ we find $\gamma = 1.291(45)$. Estimates for the critical exponents for $h_q = 0.1, 1.0$ are tabulated in Table 1. We find evidence that at small $h_q > 0$, the second-order phase transition for $q = 4$ turns into a BKT transition. For example, for $q = 4$ with $h_q = 0.1$, we find that the magnetic susceptibility diverges with volume whereas the specific heat plateaus. For $q = 2$, our results are generally consistent with a transition of the 2D Ising universality class at both $h_q = 0.1$ and $h_q = 1$.

In Fig. 3, we present scenarios of the phase diagram for small h_q (left panel) and intermediate h_q (right panel). For noninteger q, we believe the phase diagram seen in the clock model limit ($h_q \to \infty$) persists to all finite h_q with a crossover at small β and an Ising phase transition at larger β. For integer $q \geq 5$, there are two BKT transitions in the clock model limit, and these persist also to finite h_q. For integer $q = 2, 3, 4$, there is a second-order transition in the clock model limit. As the coupling h_q is reduced, the critical exponents for $q = 3, 4$ vary with h_q. We find evidence that the second-order transition for $q = 4$ turns into a BKT transition at small h_q.

4. Summary

We studied the effect of explicitly broken symmetries in classical O(2) spin systems in $(1 + 1)$ dimensions by adding a symmetry-breaking term $-h_q \sum_x \cos(q\varphi_x)$ to the ordinary O(2) model. The O(2) model is a nontrivial limit of the Abelian-Higgs model, which is a candidate for quantum simulation, and this study allowed us to explore the role of symmetry in such models. Furthermore,

PoS(LATTICE2023)223

this model allows us to interpolate between different q-state clock models, and this may be relevant for optimizing the approximation of U(1) gauge theories by $\mathbb{Z}_q$ discrete degrees of freedom.

We find a rich phase diagram with crossovers, second-order phase transitions of various universality classes, and BKT transitions. When $h_q > 0$, the O(2) symmetry is broken down to a $\mathbb{Z}_q$ symmetry, and in the limit $h_q \to \infty$, the model reduces to the q-state clock model. By continuously varying the parameter q, we are able to interpolate between different q-state clock models. The phase diagram in this clock model limit was established in Refs. [6, 7], and is illustrated in Fig. 1. For noninteger q, we found a crossover at small β, and an Ising phase transition at larger β.

In the present work, we studied the phase diagram at finite h_q using Monte Carlo and tensor renormalization group methods. For noninteger q, we found that the phase diagram in the clock model limit ($h_q \to \infty$) seems to persist to all $h_q > 0$. For integer $q \geq 5$, there are two BKT transitions in the clock model limit, and these also appear to persist to all $h_q > 0$. For $q = 2, 3, 4$, there is a second-order phase transition in the clock model limit. As h_q is decreased, we found that the critical exponents for $q = 3, 4$ vary with h_q. For $q = 4$, we found evidence that the second-order transition turns into a BKT transition at small h_q. More details can be found in our recently posted preprint [5].

Acknowledgements

This work was supported in part by the U.S. Department of Energy (DOE) under Award Numbers DE-SC0010113, and DE-SC0019139. J.Z. is supported by NSFC under Grants No. 12304172 and No. 12347101, Chongqing Natural Science Foundation under Grant No. CSTB2023NSCQ-MSX0048, and Fundamental Research Funds for the Central Universities under Projects No. 2023CDJXY-048 and No. 2020CDJQY-Z003. This research used resources of the Syracuse University HTC Campus Grid and NSF award ACI-1341006 and the National Energy Research Scientific Computing Center (NERSC), a U.S. Department of Energy Office of Science User Facility located at Lawrence Berkeley National Laboratory, operated under Contract No. DE-AC02-05CH11231 using NERSC awards HEP-ERCAP0020659 and HEP-ERCAP0023235. This work was also supported in part through computational resources and services provided by the Institute for Cyber-Enabled Research at Michigan State University.

References

[1] A. Bazavov, Y. Meurice, S.-W. Tsai, J. Unmuth-Yockey and J. Zhang, *Gauge-invariant implementation of the Abelian Higgs model on optical lattices*, *Phys. Rev.* **D92** (2015) 076003 [1503.08354].

[2] J. Zhang, J. Unmuth-Yockey, J. Zeiher, A. Bazavov, S.W. Tsai and Y. Meurice, *Quantum simulation of the universal features of the Polyakov loop*, *Phys. Rev. Lett.* **121** (2018) 223201 [1803.11166].

[3] Y. Meurice, *Examples of symmetry-preserving truncations in tensor field theory*, *Phys. Rev. D* **100** (2019) 014506.

PoS(LATTICE2023)223

[4] Y. Meurice, *Theoretical methods to design and test quantum simulators for the compact Abelian Higgs model*, *Phys. Rev. D* **104** (2021) 094513.

[5] L. Hostetler, R. Sakai, J. Zhang, A. Bazavov and Y. Meurice, *Symmetry breaking in an extended O(2) model*, *(in preparation)* (2023) [2312.xxxxx].

[6] L. Hostetler, J. Zhang, R. Sakai, J. Unmuth-Yockey, A. Bazavov and Y. Meurice, *Clock model interpolation and symmetry breaking in O(2) models*, *Phys. Rev. D* **104** (2021) 054505.

[7] L. Hostetler, J. Zhang, R. Sakai, J. Unmuth-Yockey, A. Bazavov and Y. Meurice, *Clock model interpolation and symmetry breaking in O(2) models*, *PoS(LATTICE2021)353* (2021) [2110.05527].

[8] J.V. Jose, L.P. Kadanoff, S. Kirkpatrick and D.R. Nelson, *Renormalization, vortices, and symmetry-breaking perturbations in the two-dimensional planar model*, *Phys. Rev. B* **16** (1977) 1217.

[9] T.-L.H. Nguyen and V.T. Ngo, *Study on the critical properties of thin magnetic films using the clock model*, *Advances in Natural Sciences: Nanoscience and Nanotechnology* **8** (2017) 015013.

[10] D. Landau, *Non-universal critical behavior in the planar XY-model with fourth order anisotropy*, *Journal of Magnetism and Magnetic Materials* **31-34** (1983) 1115.

[11] G. Hu and S. Ying, *Monte Carlo and coarse graining renormalization studies for the XY model with cubic anisotropy*, *Physica A: Statistical Mechanics and its Applications* **140** (1987) 585.

[12] E. Rastelli, S. Regina and A. Tassi, *Monte Carlo simulation of a planar rotator model with symmetry-breaking fields*, *Phys. Rev. B* **69** (2004) 174407.

[13] E. Rastelli, S. Regina and A. Tassi, *Monte Carlo simulation for square planar model with a small fourfold symmetry-breaking field*, *Phys. Rev. B* **70** (2004) 174447.

[14] A. Taroni, S.T. Bramwell and P.C.W. Holdsworth, *Universal window for two-dimensional critical exponents*, *Journal of Physics: Condensed Matter* **20** (2008) 275233.

[15] A. Chlebicki and P. Jakubczyk, *Criticality of the O(2) model with cubic anisotropies from nonperturbative renormalization*, *Phys. Rev. E* **100** (2019) 052106.

[16] L. Hostetler, R. Sakai, J. Zhang, J. Unmuth-Yockey, A. Bazavov and Y. Meurice, *Symmetry breaking in an extended-O(2) model*, *PoS(LATTICE2022)014* (2022) [2212.06893].

[17] L. Hostetler, *Symmetry Breaking and Clock Model Interpolation in 2D Classical O(2) Spin Systems*, phd thesis, Michigan State University, East Lansing, MI, August, 2023.

[18] H. Bernien, S. Schwartz, A. Keesling, H. Levine, A. Omran, H. Pichler et al., *Probing many-body dynamics on a 51-atom quantum simulator*, *Nature* **551** (2017) 579 [1707.04344].

PoS(LATTICE2023)223

[19] A. Keesling et al., *Quantum Kibble–Zurek mechanism and critical dynamics on a programmable Rydberg simulator*, *Nature* **568** (2019) 207 [1809.05540].

PoS(LATTICE2023)223